Ecotoxicology (2019) 28:869–877
https://doi.org/10.1007/s10646-019-02083-5

Check for updates

Physiological effects of zero-valent iron nanoparticles in rhizosphere on edible crop, *Medicago sativa* (Alfalfa), grown in soil

Jae-Hwan Kim[1] · Daniel Kim[1] · Sung Man Seo[1] · Daeyoung Kim[2]

Accepted: 16 July 2019 / Published online: 7 August 2019

Abstract

We investigated the effects of nanoscale zero-valent iron (nZVI) that has been widely used for groundwater remediation on a terrestrial crop, *Medicago sativa* (Alfalfa), and comprehensively addressed its development and growth in soil culture. Root lengths, chlorophyll, carbohydrate and lignin contents were compared, and no physiological phytotoxicity was observed in the plants. In the roots, using an omics-based analytical, we found evidence of OH radical-induced cell wall loosening from exposure to nZVI, resulting in increased root lengths that were approximately 1.5 times greater than those of the control. Moreover, germination index (GI) was employed to physiologically evaluate the impact of nZVI on germination and root length. In regard to chlorophyll concentration, nZVI-treated alfalfa exhibited a higher value in 20-day-old seedlings, whereas the carbohydrate and lignin contents were slightly decreased in nZVI-treated alfalfa. Additionally, evidence for translocation of nZVI into plant tissues was also found. Vibrating sample magnetometry on shoots revealed the translocation of nZVI from the root to shoot. In this study, using an edible crop as a representative model, the potential impact of reactive engineered nanomaterials that can be exposed to the ecosystem on plant is discussed.

Keywords Nano · Iron nanoparticle · Root · Elongation · Cell wall loosening · Phytotoxicity · Alfalfa

Introduction

Because engineered nanomaterials (ENMs) are used globally and the amount of commercial production is increasing, concern regarding the release of ENMs into the environment has also increased (Solaniki et al. 2015). Due to their unique physicochemical features such as size and reactivity, there is considerable debate over the risks of ENMs on living organisms such as plants, microorganisms, and fish. Among these, plants have received great attention since they play a crucial role in ecosystems as primary producers in the food chain. Although many researchers have performed assessments on the effects of ENMs on plants, limitations persist because most studies have been conducted in simulated environmental conditions such as hydroponic systems, not in actual environmental settings such as soil.

Nanoscale zero-valent iron (nZVI) is one of the most popular ENMs in environmental engineering that has been used for more than three decades for groundwater remediation. It has demonstrated outstanding performance, distinguished from its micron-size counterparts such as in situ chemical reduction (ISCR) reagents (Fan et al. 2016). With regard to its release into the ecosystem, nZVI is the only ENM injected underground at bulk scales and can spread to unconfined aquifers. This injection implies that terrestrial organisms, including plants, are possibly exposed to nZVI. In addition, Dwivedi et al. (2018) reported that nZVI can be adsorbed by the edible crop *Cucumis sativus* and is distributed in roots and shoots as transformed ferric citrate (hydroxyl-carboxylate product).

In previous studies, some reports address the physiological effects of iron nanoparticles (NPs) on plants, where seed germination, root elongation, or chlorophyll content were used as indicators of iron NPs toxicity (El-Temsah and Joner 2012; Lee et al. 2010; Ma et al. 2013; Barrena et al. 2009; Ghafariyan et al. 2013). Barrena et al. (2009) showed that nano-iron oxides slightly decreased the germination rate of cucumber, and Ghafariyan et al. (2013) demonstrated that

✉ Jae-Hwan Kim
jaehwankim@kigam.re.kr

[1] Advanced Geo-materials R&D Department, Pohang Branch, Korea Institute of Geoscience and Mineral Resources, Pohang 37559, Republic of Korea

[2] Department of Nanomaterials Science and Engineering, University of Science and Technology, Daejeon, Republic of Korea

soybeans exposed to superparamagnetic iron oxide NPs increased the chlorophyll level with no trace of toxicity. Most studies in the literature were conducted using hydroponic systems. Although hydroponic systems have the advantage of easily controlling experimental conditions, such as the iron NPs concentration in water, it is desirable to utilize soil systems to understand the interaction between plants and ENMs in the ecosystem, because soil systems more accurately represent actual environmental conditions. However, only a few studies utilize soil systems to evaluate the effects of iron NPs on plants (Lowry et al. 2012; Morrissey and Guerinot 2009). Lowry et al. (2012) discussed mobility reduction of iron NPs in subsurface matrix composed of larger particles such as clay in terms of heteroaggregation. Morrissey and Guerinot (2009) introduced strategies how some plants uptake Fe ion from insoluble Fe oxides in rhizosphere by expressing their genes (i.e. Arabidopsis). Therefore, in the present study, *Medicago sativa* (alfalfa), a livestock feed, was grown in soil mixed with nZVI, and its growth and development was evaluated in regard to root length, germination index, chlorophyll concentration, composition of carbohydrates and nZVI uptake. Our findings reveal the comprehensive effects of iron based ENM on the development of edible crop in soil system. Especially, to our best knowledge, this is the first study that reports nZVI-mediated cell wall loosening may occur in the natural environment.

Materials and methods

Nano zero-valent iron (nZVI) and soil

In order to investigate the effects of nZVI on root development, commercial nZVI, Reactive Nano-scale Iron Particle (RNIP), was purchased from Toda Inc. (Japan). The X-ray diffraction (XRD) pattern of nZVI was determined using PANalytical X'Pert PRO diffractometer (the Netherlands) with Cu Kα radiation (40 kV, 30 mV). The bed soil (Hungnong Co., Korea) was mainly composed of coco peat (47%), peat-moss (35%), vermiculite (10%), zeolite (7%), and caldolomite (0.6%). To prepare one pot of nZVI soil, 10 mg/110 ml of RNIP slurry and 90 g of autoclaved dry soil were mixed, using a propeller mixer, operated at 200 rpm for 10 min. The initial water content and pH of the soil were 60–70% and 5.7–6.0, respectively. Alfalfa (*Medicago sativa*) seeds were sterilized in a 2% sodium hypochlorite (Daejung, Korea) solution for 5 min and rinsed three times with autoclaved deionized water. The sterilized seeds were germinated in the soil and grown in a greenhouse under 22 °C and 16/8 h day/night conditions. For the planting and growing of alfalfa, tap water was used to reflect actual irrigation conditions and deionized (DI) ultrapure water prepared using a Barnstead purification system was used only for washing nZVI. Transmission electron microscopy (TEM) images of RNIP used in this study was obtained by using JEOL 1011 at 80 kV (Japan).

Mass spectrometry

To compare degree of polymerization (DP) of pectin-polysaccharides in root cell wall of plant treated by nZVI and control groups, the extracted root-derived polysaccharides (RDP) was prepared, and mass analysis was carried out according to previous study (Kim et al. 2014). Matrix assisted laser desorption/ionization-tome-of-flight mass spectrometry (MALDI-TOF MS), Bruker ultraflexXtreme system (Germany) was used. Each acquired spectrum represented the combined signal from 800 laser shots at each of 3 random locations on a spot, totaling 2400 laser shots, by using a 1 kHz laser. 2,5-Dihydroxybenzoic acid (Sigma-Aldrich, USA) was used as a matrix for positive modes. For MALDI analysis, the RDP solution was spotted onto a stainless steel target plate, followed by addition of matrix solution. MALDI-TOF MS via collision-induced dissociation was then performed for selected peaks in the positive ion mode. Tandem MS spectra were obtained at 1 kV collision energy with argon gas.

Germination index

Since germination index (GI) is one of the most representative parameters frequently used in phytotoxicity researches, employed in the present study as well. The GI of 10-day-old alfalfa was determined according to the following standard method, which has been used as a guideline to evaluate the phytotoxicity of superparamagnetic iron oxide NPs (SPIONs) in by the United States EPA and OECD (Ghafariyan et al. 2013).

- Relative root elongation (RE) = Mean root length with NPs/Mean root length with control × 100%
- Relative root germination (RG) = Seeds germinated with NPs/Seeds germinated with control × 100%
- Germination index (GI) = RE × RG/100%

DCFH-DA assay

2′,7′-dichlorofluorescine-diacetate (DCFH-DA) assay was conducted to detect the presence of OH radicals on the surface of nZVI particles following by previous study with little modification (Meng et al. 2012). nZVI particles were incubated in 2 μM DCFH-DA solution (Sigma Aldrich, USA) for 10 min. After that, rinsed three times with 10 mM PBS buffer at pH 7.4 and deionized water. Emission and

excitation wavelength were 488 nm and 505–530 nm, respectively (Zeiss Axioplan, Germany)

Phytotoxicity assay

GI and chlorophyll concentration were selected as phytotoxicity parameters to determine the effect of nZVI on plant growth. For GI, RG was calculated from 5-day-old seedlings, because the emergence of coleoptile for alfalfa was observed to appear after 5 days. For comparison of chlorophyll concentration, Fe(II)-EDTA-treated soil was newly added ($FeSO_4$•$7H_2O$ (Daejung, Korea), EDTA (Junsei, Japan)). Fe(II)-EDTA-treated soil was prepared according to the same method as the nZVI soil. Concentrations of Fe (II)-EDTA was 0.5 g per 1 kg of soil. For the Fe(II)-EDTA solution, the molar ratio of Fe(II) and EDTA was 1:1. Chlorophyll concentrations were measured for all plant leaves at day 7, 10, and 20. For 10 and 20-day-old seedlings, subapical leaves were harvested for measurement. Chlorophyll was extracted with 2 ml of 95% ethanol (v/v) for 10 h at room temperature, which was then measured using a Cary 50 UV spectrophotometer at 645 and 663 nm (Varian, USA). The chlorophyll A and B contents were calculated according to the method of Vernon (1960).

Measurement for plant-available Fe in soil

Plant-available Fe in soil was measured according to the method described by Walker et al. (2003), with minor modification. A DTPA (diethylenetriaminepentaacetic acid, Sigma-Aldrich, USA) extraction solution was prepared by dissolving 492 mg of DTPA in 250 ml of 1 mM $CaCl_2$ (Daejung, Korea) solution with a pH of 7.3. 20 ml of DTPA solution was poured into glass Erlenmeyer flasks containing 2.5 g of oven dried soil pulverized to pass through a 10-mesh sieve (<2.0 mm). The flasks were placed on an orbital shaker for 4 h at 200 rpm and 30 °C, followed by filtration using Whatman B5 filter papers. Inductively coupled plasma mass spectrometer (ICP-OES, Thermo Scientific, USA) was used to measure Fe concentrations. All analyses were performed in triplicate.

Uptake of nZVI inside plant tissues

To detect the distribution of nZVI inside plant tissues, magnetic measurement was conducted using a superconducting quantum interfere device magnetometer (Quantum Design, MPMS-XL 7, USA). To remove soil attached to the plants, 28-day-old seedlings were washed with deionized water and divided into the following: roots, crowns, and stems. Each dried tissue was ground using a mortar and pestle to fine particle size and 20 mg of samples were obtained. Magnetization was determined under an applied field ranging from −8 to 8 T.

Carbohydrate and lignin content in plants

The composition of carbohydrates and lignin in plants was measured in accordance with the Klason method, adopted from the Laboratory Analytical Procedures for standard biomass analysis provided by the National Renewable Energy Laboratory (NREL) (Ning et al. 2016). Overnight, 20-day-old seedlings were dried in an oven at 105 °C, and 0.3 g of dried sample was dissolved in 3 ml of 72% sulfuric acid and shaken for 2 h at 30 °C. To compensate for the loss of water, 84 ml of DI water was added to the vial and the water loss was compared using another 87 ml of DI water. The sample was neutralized to pH 6–7 with 0.1 M $CaCO_3$ (Daejung, Korea) before being centrifuged for 10 min at 15,000 rpm. Concentrations of sugars such as glucose and xylose in the supernatants were quantitatively measured using high-performance liquid chromatography (HPLC, Agilent, USA). For the lignin content, all the solids remaining at the bottom of the filtering crucible were carefully collected and washed with deionized water. The residue in the crucible was dried overnight in an oven at 105 °C (W_{r+c}). The dry sample and crucible were oxidized together in a muffle furnace at 575 °C for 6 h to determine the ash content in the residue (W_a). The total lignin content was $(W_{r+c} - W_c - W_a)$/(total dry alfalfa weight (0.3 g)) × 100%, where W_c is the oven dry weight of the crucible. All analyses were performed in triplicate.

Results and discussion

Effects of nZVI on root growth

Figure 1a, b show the TEM image of nZVI used in the experiment and the phenotype images of 10-day-old alfalfa harvested from two groups of soil, respectively. In the plant's aerial portion, there was no significant difference or toxicity observed on the growth of the alfalfa's cotyledons exposed to nZVI compared to that of the control, such as senescence. However, the roots exposed to nZVI exhibited enhanced root lengths compared to that of the control, measuring on average approximately 150% longer (3.1 ± 0.7 vs 5.0 ± 1 cm). As presented Table 1, the GI value of alfalfa grown in the nZVI soil was on average 50% higher than that of the control. This result indicates that the presence of nZVI in rhizosphere positively affects the growth of root in phytotoxicity. Especially, RE was a critical factor in evaluating GI values in this study, because there was no significant difference in the RG between the two groups.

As one of component of cell wall, pectin-polysaccharides are networking polymers and load-bearing hexose. The degradation of pectin-polysaccharides (breakdown of networking polymers), called cell wall loosening, is necessary

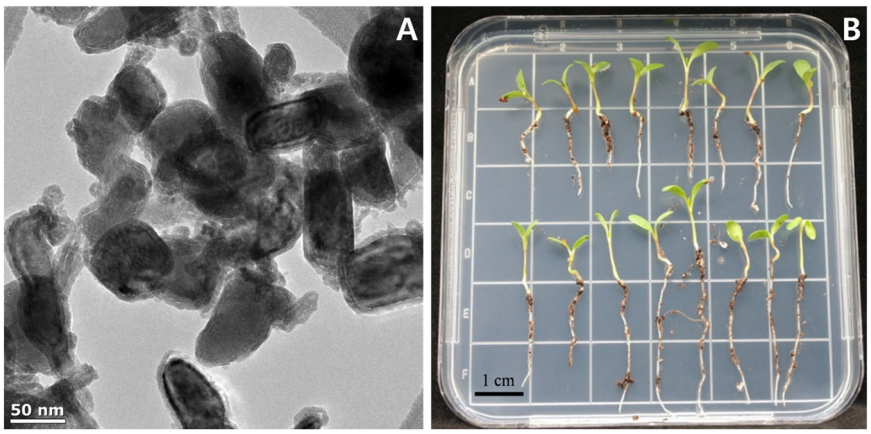

Fig. 1 **a** TEM image of nZVI particles used in the present study, **b** image of 10-day-old alfalfa grown in soil, in which the plants exposed to nZVI (bottom) exhibited better root elongation than that of the control (top)

Table 1 Germination index (GI) of alfalfa grown in nZVI soil for 10 days

Seedling (16 seeds)	Relative root germination (RG)	Relative root elongation (RE)	GI (RG × RE/100)
Exp. 1	90	142	128
Exp. 2	125	120	150
Exp. 3	100	190	190
Mean	105	151	156

for plant growth and development because cell wall functions as exoskeleton of cytoplasm (An et al. 2005; De Varies and Visser 2001; Voragen et al. 2009). In our previous study, OH radical-induced cell wall loosening by nZVI was firstly demonstrated through in vivo profiling of pectin-polysaccharides in cell walls, degradation of pectin-polysaccharides with lower DP was detected in MALDI-TOF MS (Kim et al. 2014). Therefore, in the present study, the MALDI-TOF MS profiles of pectin-polysaccharides obtained from alfalfa were compared to confirm that the enhanced root elongation resulted from OH radical-induced cell wall loosening and whether it was able to occur in soil culture. The distribution of the polysaccharides and chromatogram of the MALDI-TOF MS results are presented in Fig. 2. The DP ranged from 4 to 12 in the control, whereas a relatively lower DP up to 8 was observed in the alfalfa grown in the soil mixed with nZVI. These data reveal that the pectin-polysaccharides in the root cell walls were degraded by nZVI in rhizosphere.

Schopfer (2001) reported OH radical can mediate cell-wall loosening for elongation of growth. The OH radicals are very reactive so that can act as scissors to breakdown the network of pectin-polysaccharides in the cell walls. This results in much longer root length by reducing cell wall stress, named OH radical-induced cell wall loosening. In the literature, it is readily found that nZVI is capable of generating reactive oxygen species (ROS) such as H_2O_2 or OH radical via Fenton-like or Haber–Weiss reaction as followings (Sung et al. 2005; Pignatello et al. 2006). In our study, with DCFH-DA assay, the presence of ROS (H_2O_2 or OH radicals) on the surface of nZVI was proven and its confocal microscopy images were shown in Fig. 3. On the basis of mechanisms DCFH oxidation occurred by action of H_2O_2 in the presence of metallic catalyst such as Fe(II), OH radical is a species responsible for the oxidation (Zhu et al. 1994; Myhre et al. 2003; Gomes et al. 2005). Therefore, this result suggests that nZVI treatment is possible to cause the production of ROS such as H_2O_2 or OH radical in rhizosphere via the metallic catalyst, resulting in OH radical-induced cell wall loosening in plant tissue (Kim et al. 2014).

$$Fe^0 + O_2 + 2H^+ \rightarrow Fe^{2+} + H_2O_2 \quad (1)$$

$$Fe^0 + H_2O_2 \rightarrow Fe^{2+} + 2OH^- \quad (2)$$

$$Fe^{2+} + H_2O_2 \rightarrow Fe^{3+} + OH\bullet + 2OH^- \quad (3)$$

In terms of nano-phytotoxicity, the finding is very meaningful and interesting because same phenotype—root elongation—was expressed not only in Arabidopsis but also in other plant species, which means OH radical-induced cell wall loosening by nZVI is able to occur regardless of species-specificity. The phenotypic effects of metal NPs have been known to vary from species to plants in general. Some NPs such as ZnO and CeO_2 differentially affected root elongation of soybean (López-Moreno et al. 2010). CeO_2 concentrations significantly increased root elongation but ZnO significantly decreased root growth. In another study, nano-CeO_2 had no effect on the root elongation of six plants but inhibited the root elongation of lettuce (Ma et al. 2010). Besides, it was found that Fe_3O_4 NPs can inhibit the root elongation of Arabidopsis (Lee et al. 2010), but pumpkin showed significantly increased root length (Wang et al. 2011). Therefore, even though alfalfa cannot represent

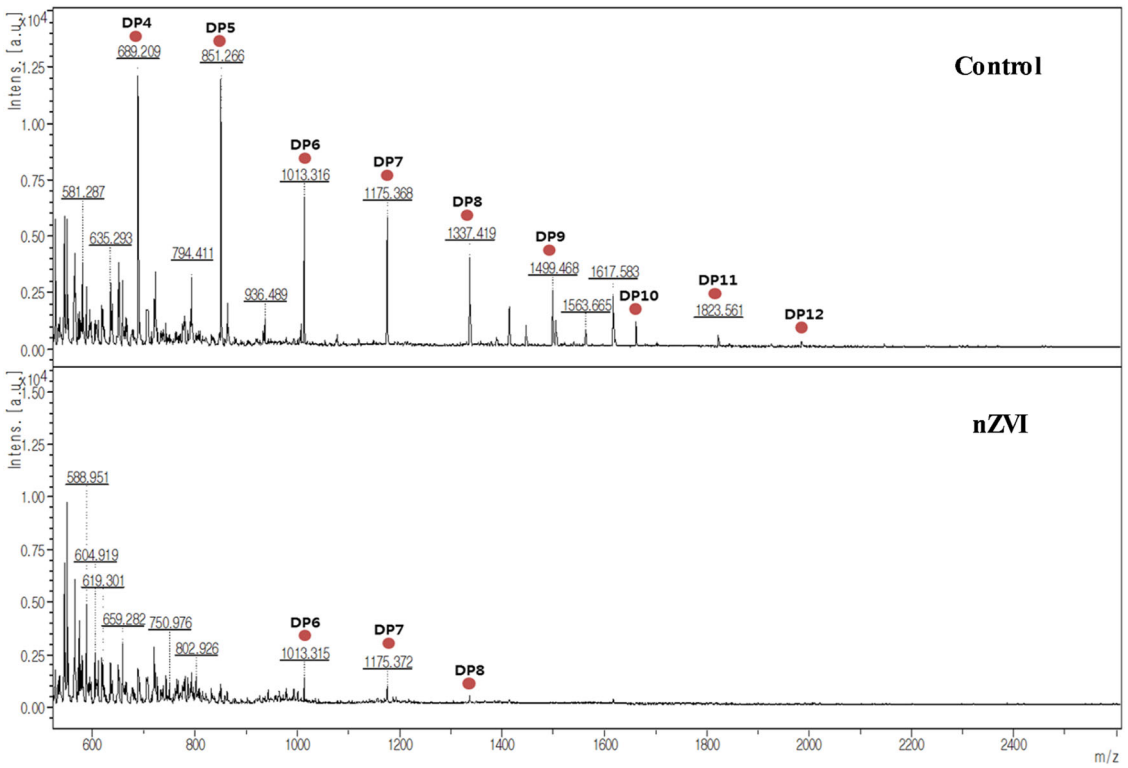

Fig. 2 Matrix assisted laser desorption/ionization time of flight mass spectrometry (MALDI-TOF MS) spectrum of root-derived polysaccharide oligomers from the control alfalfa (top) and nZVI-treated alfalfa (bottom)

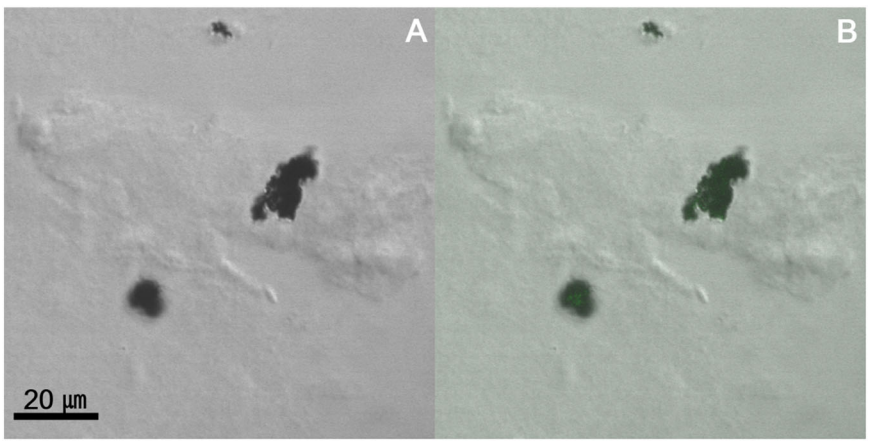

Fig. 3 Confocal microscopy image for the presence of OH radical on the surface of nZVI particles obtained by DCFH-DA staining. **a** Bright field, **b** Mergence

all plants, the present findings provide meaningful information and fill the knowledge gap to better understand the impact of ENMs on plants.

Evidence for the uptake and translocation of iron NPs inside plants

To detect whether nZVI was translocated in plant tissues, dried and powdered root, crown, and stem samples from 28-day-old alfalfa seedlings were subjected to magnetic measurement using a superconducting quantum interfere device magnetometer. Figure 4 shows the results of the measured magnetization of different tissues from the nZVI-treated alfalfa. All signals were in measurable range, whereas no magnetization signals (data not shown) were detected in tissues of the control plants within the detection limit (>1 µemu/g). Inserts in Fig. 4 present a magnified view of the magnetization in tissues at a low applied field range from −3000 to 3000 Oe, clearly showing that magnetization increased as the applied field increased with a positive slope in the field region. Although scattering was observed in the stem, the main tendency was toward an increase in the

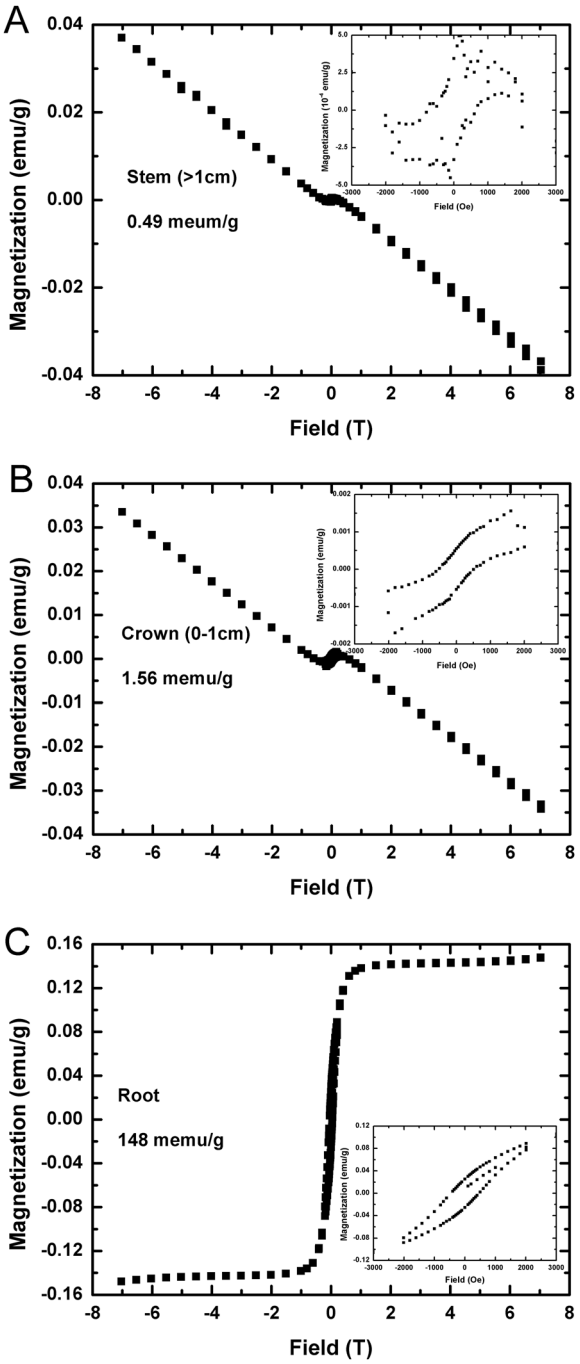

Fig. 4 Selected vibrating sample magnetometer (VSM) curves of alfalfa **a** stem, **b** crown, and **c** root indicating the presence of nZVI in plant tissues. Inserts are magnification of the magnetization from −3000 to 3000 Oe (10,000 Gauss = 1 T)

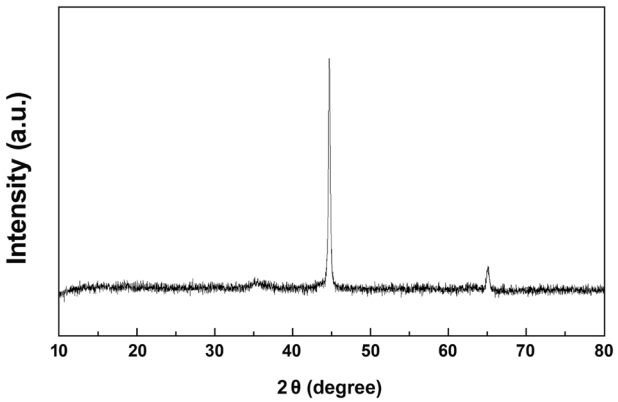

Fig. 5 X-ray diffraction (XRD) pattern of nZVI particles

applied range. The magnetization value of the root was 2 or 3 orders higher than that of the crown and stem. Yet, we still do not know the exact transformed products of nZVI in the tissue with the only magnetization analysis, even though the degree of magnetization signal detected in Fig. 4 showed similarity to that of iron NPs such as magnetite (Zhu et al. 2008). According to recent studies, nZVI or nano magnetite are known to be transformed in plant tissues to Fe-citrate complexes similarly (Wang et al. 2011; Ghafariyan et al. 2013). However, Fe-citrate was found to have no magnetization, the magnetization observed in plant root was figured out to be induced from iron oxyhydroxides such as maghemite or lepidocrocite by synchrotron-based X-ray absorption technology such as near-edge X-ray absorption fine structure (NEXAFS) or extended X-ray absorption fine structure (EXAFS) measurements (Dwivedi et al. 2018). Thus, we concluded that the magnetization signals shown in Fig. 4 possibly resulted from iron oxyhydroxides. However, the previous studies were carried out hydroponically, further study for plant grown in soil should be needed to perform using X-ray absorption technology.

In the case of NPs including nZVI, the exact uptake or translocation mechanism in plant tissues has yet to be determined, with theories such as plasmodesmata, osmotic pressure, lignin content, and endocytosis (Lin and Xing 2008; Nowack and Bucheli 2007; Ma et al. 2013; Kim et al. 2014). Recently, it was suggested that plasmodesmo plays an important role in transporting Au NPs into plant bodies as the presence of NPs in plasmodesmata was experimentally proven (Zhai et al. 2014). Plasmodesma is microscopic channels between cell walls and known to have about 50–60 nm diameter (Robards 1975). In Fig. 1a, although the nZVI particles are shown to be aggregated each other, but based on the XRD result (Fig. 5), the average particle size of nZVI obtained from Scherrer's formula ($2\theta = 44.6°$) was 55 ± 1 nm. Ma et al. (2013) reported that the permeability of foreign materials in the cells increases in parallel with the decrease of lignin content in plants. In the case of *Poplar*, which has relatively low lignin contents in cell walls compared to *Typha*, nZVI was observed in root cells. Table 2 presents the composition of carbohydrates, such as glucose, xylose, and lignin, in plants grown in the control soil and nZVI soil. In the roots, a significant decline of all three components was observed, in which lignin content was reduced the most (22%) among the three component,

Table 2 Glucose, xylose, and lignin composition in two plant groups (20-day-old). The obtained values from analysis are means, and all experiment were conducted in triplicate. Different letters represent significant differences among the different group ($P < 0.05$, Student's *t* test)

Tissue	Group	Soluble sugar (%)		Lignin (%)
		Glucose	Xylose	
Shoot	Control	16.1 ± 1.2	5.3 ± 0.5	14.9 ± 2.6
	nZVI	15.6 ± 1.4	5.2 ± 0.8	15.0 ± 1.6
Root	Control	14.9 ± 2.5[a]	4.9 ± 0.9[a]	25.9 ± 1.4[a]
	nZVI	12.8 ± 3.1[b]	4.5 ± 0.1[b]	20.2 ± 2.7[b]

glucose and xylose were reduced by approximately 14 and 8%, respectively. Besides, endocytosis is known to be one of possible ENMs uptake processes of plants (Rastogi et al. 2017; Lv et al. 2019). Root where OH radical-induced cell wall loosening occurred showed increased endocytosis (Kim et al. 2014). Because, cell that has relatively reduced mechanical strain on cell wall possibly increases endocytosis in respect to cell polarity (Li et al. 2012), and OH radical-induced cell wall loosening is accompanied by stress relaxation (Schopfer 2006).

According to previous study, not only iron NPs size but also water permeability of cultural media affected translocation of NPs. Zhu et al. (2008) grew pumpkins in soil and sand by irrigating a nano-magnetite suspension periodically, demonstrating that measurable magnetic signals were detected in plants that were only grown in sand. Because sand typically has a larger porosity and hydraulic conductivity than soil, the mobility of nano-magnetite suspensions in sand is likely to be higher than that in soil, which can cause NPs to easily reach the rhizosphere when a NPs suspension is irrigated, eventually allowing NPs to be adsorbed by roots. In other words, in terms of NP mobility, supplying plants grown in soil with a NP suspension was not a suitable means for providing enough contact area to roots due to low permeability (Saleh et al. 2007). From this perspective, the bed soil used as cultural media in this study was able to increase nZVI mobility in the rhizosphere with sufficient water permeability. Taken together, the nZVI particles are possibly to be penetrated into the cell walls and located in body of plant. However, there is still debate for the uptake and translocation of NPs to plant tissue, further study to better understand the mechanisms involved for the issue should be performed in the near future.

Comparison of concentrations chlorophyll and Fe ion released in soil

Although there are several factors that determine the kinetic release of the Fe ion from iron NPs such as chemical composition, surface charge, and redox-potential,

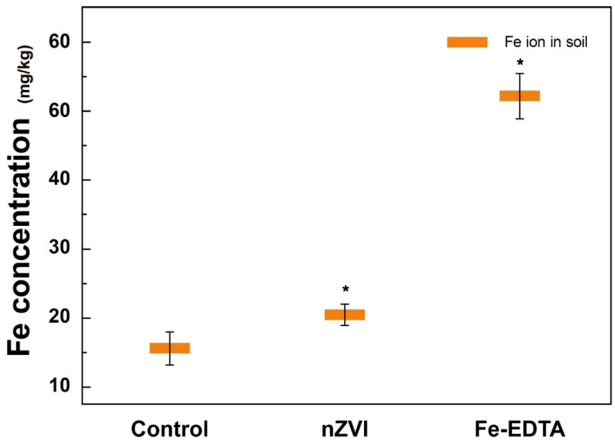

Fig. 6 Concentration of plant-available Fe ion in each soil. Compared to that of nZVI soil, the concentration of plant-available Fe of the control is slightly lower, but that of Fe-EDTA soil is approximately 5 times more than that of the control. Symbols represent means and error bars represent 95% confidence intervals. Significant differences relative to the controls ($P < 0.05$) are marked with asterisks (Student's *t* test)

cultivation modes are the most important. For example, germination was only inhibited at 250 mg/L of nZVI in a hydroponic system, whereas 1 g/kg nZVI was required for the same inhibition in a soil system (El-Temsah and Joner 2012). Therefore, to examine how much Fe ion was released into the soil from nZVI, the DTPA method was employed to measure the plant-available Fe. Figure 6 shows the plant-available Fe concentration of three groups—the control, nZVI-, and Fe(II)-EDTA treated soil—which were 15.6 ± 1.0, 20.5 ± 1.4, and 52.2 ± 0.4 mg/kg, respectively. There is statistically significant difference between control and each experimental groups (Student's *t* test, $P < 0.05$).

As shown in Fig. 7, alfalfa grown in nZVI soil exhibited a higher chlorophyll concentration compared to the other two groups during experimental period. However, in case of alfalfa grown in Fe(II)-EDTA soil, both a lower chlorophyll concentration and germination rate (90.6 %) were observed, which is believed to be due to excess Fe ions and its lower tolerance. In Fig. 6, the Fe concentration of the nZVI-treated soil was only slightly higher than that of the control, whereas the Fe concentration of the Fe(II)-EDTA-treated soil was more than 3 times that of the control. Our findings were consistent with a previous study that described a relatively slow release of Fe ion from nano-magnetite (Ghafariyan et al. 2013); the Fe ion concentration range induced by the nZVI soil treatment was tolerable to alfalfa and suitable for chlorophyll production. In 10 and 20-day-old seedling, there is also statistically significant difference between control and each experimental groups (Student's *t* test, $P < 0.05$).

As one of photosynthetic pigments, chlorophyll has been paid attention in NPs toxicity studies. In case of iron NPs

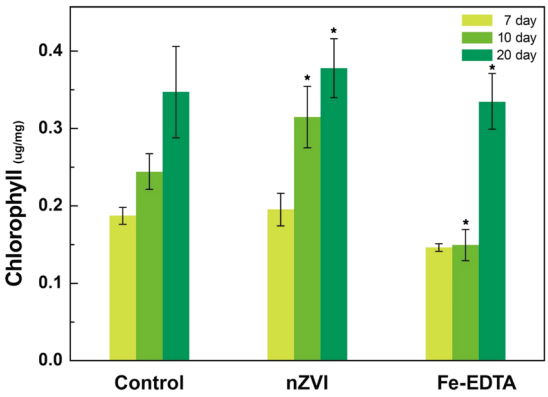

Fig. 7 Chlorophyll concentration in subapical leaves of alfalfa grown in the control, nZVI-treated, and Fe-EDTA soil. Symbols represent means and error bars represent 95% confidence intervals. Significant differences relative to the controls ($P < 0.05$) are marked with asterisks (Student's t test)

Table 3 Raw data for chlorophyll a and b of all groups in 20-day-old seedlings. The obtained correlation coefficient from those data is over 0.9

Group	Chlorophyll a	Chlorophyll b	Chlorophyll a/b
Control	7.30	0.72	10.14
	5.33	0.54	9.87
	4.82	0.52	9.27
nZVI	5.90	0.59	10
	6.03	0.61	9.89
	5.28	0.57	9.26
Fe-EDTA	4.56	0.46	9.91
	3.43	0.35	9.80
	7.79	0.92	8.47
Correlation coefficient	$R^2 = 0.935$ (X = Chlorophyll a, Y = Chlorophyll b)		

with magnetization, they had affected chlorophyll content positively when they were in rhizosphere or being translocated into plant tissue without toxic symptom such as chlorosis (Racuciu and Creanga 2007; Pariona et al. 2017; Tombuloglu et al. 2019; Ghafariyan et al. 2013). Tombuloglu et al. (2019) reported that nano-magnetite inclusion in barely increased chlorophyll compared to that of control group, especially chlorophyll a increased significantly. Ghafariyan et al. (2013) suggested the possibility that nano-magnetite inclusion with magnetization could affect the biosynthesis of chlorophyll a in soybean, when there was no significant difference in the ratio of chlorophyll a/b in each groups and correlation coefficient between chlorophyll a and b was over 0.9 indicating linear correlation. Table 3 shows the values of chlorophyll a, b, and a/b of all the groups in 20-day-old seedlings. The evaluated ratio of chlorophyll a/b was almost maintained constant from 9 to 10 and the correlation coefficient was calculated over 0.9. Our finding is in parallel with that reports in the previous ones (Ghafariyan et al. 2013; Tombuloglu et al. 2019). Therefore, it can be claimed that plant-available Fe ion and iron NPs inclusion possibly contribute the increased chlorophyll concentration of alfalfa.

Conclusion

We investigated the comprehensive effects of nZVI on crop species, alfalfa, in soil system. nZVI-mediated OH radical-induced cell wall loosening was observed in the presence of nZVI in rhizosphere. Biological influence on plant growth was evaluated using representative physiological parameters of plant such as germination index, carbohydrates composition, and chlorophyll concentration. We found that root of alfalfa exposed to nZVI was elongated by the OH radical-induced cell wall loosening, which affected in GI, which is calculated using RG and RE, about 150%. Moreover, there was no toxic symptom observed in alfalfa grown in the soil mixed with nZVI. In case of nZVI uptake, although we found the evidence that nZVI can be uptaken inside of alfalfa using vibrating sample magnetometer, further investigation is needed for more direct evidence of nZVI transformed products using synchrotron-based X-ray absorption such as NEXAFS or EXAFS. The alfalfa exposed to nZVI showed higher chlorophyll concentration compared to that of the control, owing to the increased plant available Fe concentration and iron NPs inclusion induced biosynthesis of chlorophyll a. Taken together, the exposure to nZVI in soil brought various changes in plant physiology, which enhanced root elongation, germination index, and chlorophyll concentration.

Acknowledgements This research was supported by the Basic Research Project of the Korea Institute of Geoscience and Mineral Resources (KIGAM) funded by the Ministry of Science and ICT of Korea.

Compliance with ethical standards

Conflict of interest The authors declare that they have no conflict of interest.

References

Solaniki P, Bhargava A, Chhipa H, Jain N, Panwar J (2015) Nano-fertilizers and their smart delivery system. In: Rai M, Ribeiro C, Mattoso L, Duran N (eds) Nanotechnologies in food and agriculture. Springer, Switzerland, pp 81–101

Fan D, O'Brien Johnson G, Tratnyek PG, Johnson RL (2016) Sulfidation of nano zerovalent iron (nZVI) for improved selectivity

during in-situ chemical reduction (ISCR). Environ Sci Technol 50:9558–9568

Dwivedi AD, Yoon H, Singh JP, Chae KH, Rho S, Hwang DS, Chang YS (2018) Uptake, distribution, and transformation of zerovalent iron nanoparticles in the edible plant *Cucumis sativus*. Environ Sci Technol 52:10057–10066

El-Temsah YS, Joner EJ (2012) Impact of Fe and Ag nanoparticles on seed germination and differences in bioavailability during exposure in aqueous suspension and soil. Environ Toxicol 27:42–49

Lee CW, Mahendra S, Zodrow K, Li D, Tsai YC, Braam J, Alvarez PJJ (2010) Developmental phytotoxicity of metal oxide nanoparticles to Arabidopsis thaliana. Environ Toxicol Chem 29:669–675

Ma X, Gurung A, Deng Y (2013) Phytotoxicity and uptake of nanoscale zero-valent iron (nZVI) by two plant species. Sci Total Environ 443:844–849

Barrena R, Casals E, Colón J, Font X, Sánchez A, Puntes V (2009) Evaluation of the ecotoxicity of model nanoparticles. Chemosphere 75:850–857

Ghafariyan MH, Malakouti MJ, Dadpour MR, Stroeve P, Mahmoudi M (2013) Effects of magnetite nanoparticles on soybean chlorophyll. Environ Sci Technol 47:10645–10652

Lowry GV, Gregory KB, Apte SC, Lead JR (2012) Transformations of nanomaterials in the environment. Environ Sci Technol 46:6893–6899

Morrissey J, Guerinot ML (2009) Iron uptake and transport in plants: the good, the bad, and the ionome. Chem Rev 109:4553–4567

Kim JH, Lee Y, Kim EJ, Gu S, Sohn EJ, Seo YS, An HJ, Chang YS (2014) Exposure of iron nanoparticles to *Arabidopsis thaliana* enhances root elongation by triggering cell wall loosening. Environ Sci Technol 48:3477–3485

Meng L, Zhang X, Lu Q, Fei Z, Dyson PJ (2012) Single walled carbon nanotubes as drug delivery vehicles: targeting doxorubicin to tumors. Biomaterials 33:1689–1698

Vernon LP (1960) Spectrophotometric determination of chlorophylls and pheophytins in plant extracts. Anal Chem 32:1144–1150

Walker DJ, Clemente R, Roig A, Bernal MP (2003) The effects of soil amendments on heavy metal bioavailability in two contaminated Mediterranean soils. Environ Pollut 122:303–312

Ning L, Xeujun P, Jane A (2016) A facile and fast method for quantitating lignin in lignocellulosic biomass using acidic lithium bromide trihydrate (ALBTH). Green Chem 18:5367–5376

An HJ, Lurie S, Greve LC, Rosenquist D, Kirmiz C, Labavitch JM, Lebrilla CB (2005) Determination of pathogen-related enzyme action by mass spectrometry analysis of pectin breakdown products of plat cell walls. Anal Biochem 338:71–82

De Varies RP, Visser J (2001) Aspergillus enzymes involved in degradation of plant cell wall polysaccharides. Microbiol Mol Biol Rev 65:497–522

Voragen AGJ, Coenen G, Verhoef RP, Schols HA (2009) Pectin, a versatile polysaccharide present in plant cell walls. Struct Chem 20:263–275

Schopfer P (2001) Hydroxyl radical-induced cell-wall loosening in vitro and in vivo: implications for the control of elongation growth. Plant J 28:679–688

Sung HJ, Feitz AJ, Sedlak DL, Waite TD (2005) Quantification of the oxidizing capacity of nanopariticulate zero-valent iron. Environ Sci Technol 39:1263–1268

Pignatello JJ, Oliveros E, MacKay A (2006) Advanced oxidation processes for organic contaminant destruction based on the fenton reaction and related chemistry. Crit Rev Environ Sci Technol 36:1–84

Zhu H, Bannenberg GL, Moldeus P, Shertzer HG (1994) Oxidation pathways for the intracellular probe 2′,7′-dichlorofluorescein. Arch Toxicol 68:582–587

Myhre O, Anderson JM, Aarnes H, Fonnum F (2003) Evaluation of the probes 2′,7′-dichlorofluorescin diacetate, luminol, and lucigenin as indicators of reactive species formation. Biochem Pharmacol 65:1575–1582

Gomes A, Fernandes E, Lima JLFC (2005) Fluorescence probes used for detection of reactive oxygen species. J Biochem Biophys Methods 65:45–80

López-Moreno ML, de la Rosa G, Hernández-Viezcas JÁ, Castillo-Michel H, Botez CE, Peralta-Videa JR, Gardea-Torresdey JL (2010) Evidence of the differential biotransformation and genotoxicity of ZnO and CeO_2 nanoparticles on soybean (*Glycine max*). Plants Environ Sci Technol 44:7315–7320

Ma Y, Kuang L, He X, Bai W, Ding Y, Zhang Z, Zhao Y, Chai Z (2010) Effects of rare earth oxide nanoparticles on root elongation of plants. Chemosphere 78:273–279

Wang H, Kou X, Pei Z, Xiao JQ, Shan X, Xing B (2011) Physiological effects of magnetite (Fe_3O_4) nanoparticles on perennial ryegrass (*Lolium perenne L.*) and pumpkin (*Cucurbita mixta*) plants. Nanotoxicology 5:30–42

Zhu H, Han J, Xiao JQ, Jin Y (2008) Uptake, translocation, and accumulation of manufactured iron oxide nanoparticles by pumpkin plants. J Environ Monit 10:713–717

Lin D, Xing B (2008) Root uptake and phytotoxicity of ZnO nanoparticles. Environ Sci Technol 42:5580–11165

Nowack B, Bucheli TD (2007) Occurrence, behavior and effects of nanoparticles in the environment. Environ Pollut 150:5–22

Zhai G, Wlters SK, Peate DW, Alvarez PJJ, Schnoor JL (2014) Transport of gold nanoparticles through plasmodesmata and precipitation of gold ions in woody poplar. Environ Sci Technol Lett 1:146–151

Robards AW (1975) Plasmodesmata. Annu Rev Plant Physiol 26:13–29

Rastogi A, Zivcak M, Kalai HM, He X, Mbarki S, Brestic M (2017) Impact of metal and metal oxide nanoparticles on plant: a critical review. Front Chem 5:78

Lv J, Christie P, Zhang S (2019) Uptake, translocation, and transformation of metal-based nanoparticles in plants; recent advances and methodological challenges. Environ Sci Nano 6:41–59

Li H, Friml J, Grunewald W (2012) Cell polarity: stretching prevents developmental cramps. Curr Biol 22:635–637

Schopfer P (2006) Biomechanics of plant growth. Am J Bot 93:1415–1425

Saleh N, Sirk K, Liu Y, Phenrat T, Dufour B, Matyjaszewski K, Tilton RD, Lowry GV (2007) Surface modifications enhance nanoiron transport and NAPL targeting in saturated porous media. Environ Eng Sci 24:45–57

Racuciu M, Creanga D (2007) THA-OH coated magnetic nanoparticles internalized in vegetal tissue. Rom J Phys 52:395–402

Pariona N, Martinez A, Hernandez-Flores H, Clark-Tapi R (2017) Effect of magnetite nanoparticles on the germination and early growth of *Quercus macdougallii*. Sci Total Environ 575:869–875

Tombuloglu H, Slimani Y, Tombuloglu G, Almessiere M (2019) Uptake and translocation of magnetite (Fe_3O_4) nanoparticles and its impact on photosysnthetic genes in barley (*Hordeum vulgare* L.). Chemosphere 226:110–122